Progress In Electromagnetics Research M, Vol. 92, 55–65, 2020

A Novel Approach for Human Intention Recognition Based on Hall Effect Sensors and Permanent Magnets

Van Tai Nguyen[1, 2, *], Tien-Fu Lu[1], Paul Grimshaw[1], and Will Robertson[1]

Abstract—Human intention recognition is important for any interaction between the user and the exoskeleton. This study proposes a novel approach, based on a contactless sensory system, using linear Hall effect sensors to recognize human intentions. This contactless sensory system consists of four Hall effect sensors mounted on the exoskeleton, whilst a ring-shaped permanent magnet with diametrical magnetization consisting of two semi-rings is worn on the user's forearm. The model of the magnetic field created by the permanent magnet is also developed. Based on the developed magnetic field model and by interpreting the signals from the Hall effect sensory system received while the user's elbow and forearm move, the intention identification algorithm is derived. A lightweight elbow and forearm assistive exoskeleton is developed. The proposed approach for human intention recognition is used to assist in controlling the exoskeleton, following the wearer's intended motions. By implementing this contactless sensory system, wearers can use the exoskeleton easily and can move their forearm comfortably, while the human intention motion is recognized and used to control the exoskeleton. Moreover, achieved signals are unaffected by skin perspiration and muscle fatigue. As the sensory system is mounted on the exoskeleton, there is only indirect contact between the user's body and the sensors, leading to improved comfort. Finally, the system does not require expert knowledge to place the sensors on the body of the user. This approach can be extended to detect human intentions for the control of exoskeletons with more degrees of freedom.

1. INTRODUCTION

One of the important aspects in the control of a human-exoskeleton interface is to follow the user's intentions correctly and at the correct pace. There are a number of research projects attempting to develop methods of human intention recognition for the control of exoskeletons based on contact sensory systems. Rahman et al. proposed a strategic control method based on Electromyography (EMG) signals recorded from users to manoeuvre a wearable exoskeleton robot named ETS-MARSE for the rehabilitation and assistance of upper-extremity movements [1]. EMG based methods have also been found in a number of other studies [2–7]. One of the problems when using this type of method is that it requires expert knowledge to put the electrodes on the correct muscle positions on the wearer's shoulder and elbow, which is not always possible for the user themselves. Another problem is that the locations of the electrodes can change during limb movements, due to skin perspiration or the lack of effective electrode fixation forces which can cause unstable signal patterns. Consequently, the accuracy of the prediction as to the location of the electrodes can be affected. Furthermore, wearing electrodes on the body can make the user feel uncomfortable. It is also time-consuming to put all the electrodes on in the correct positions. Moreover, EMG signals could be weak and noisy, which makes the methods of processing the signals complex. As a result, the effectiveness of using the exoskeleton decreases.

Received 28 November 2019, Accepted 23 March 2020, Scheduled 6 May 2020
* Corresponding author: Van Tai Nguyen (tainv@tlu.edu.vn, vantai.nguyen@adelaide.edu.au or 88.vantai.nguyen@gmail.com).
[1] School of Mechanical Engineering, University of Adelaide, SA 5005, Australia. [2] Faculty of Mechanical Engineering, Thuyloi University, 175 Tay Son, Dong Da, Hanoi, Vietnam.

Another method of human intention recognition is based on an electroencephalogram (EEG) [8–15], a non-invasive method that has been used to recognize brain signal changes before the onset of limb movements [14]. Noda et al. [15] used recorded brain signals to control an assistive robot system following stand-up movements. However, the EEG signals are unstable because the position of the electrodes placed on the wearer's head can change during activity and cause a change in signal patterns. Moreover, patients need to pay full attention to their intended movements, which may lead to unwanted motion when they suddenly change their thoughts. Wearing electrodes can also cause discomfort, which decreases the effectiveness of using the EEG method.

Because of the disadvantages of using EMG and EEG-based techniques, many researchers have used an alternative method of human intention recognition based on force sensors. Ammar et al. [16] embedded a force sensor in a biceps ring mounted on an exoskeleton to measure the pressure exerted by the biceps on the ring. By interpreting the achieved pressure signals, human intention for motion can be predicted to control the exoskeleton. However, because the biceps need to contact the exoskeleton directly, the user's arm needs to exert a force from the exoskeleton. Therefore, the user's arm can become fatigued, decreasing the efficacy of the exoskeleton. Force myography based on force sensors has been studied by Ul Islam and Bai [17], Xiao et al. [18], and Cho et al. [19] to recognize human intentions to control prostheses. Although signal patterns, recorded from the force sensors in these studies, can be used to predict the wearer's intended motion(s), the user still needs to wear the sensory system on the body, which is uncomfortable. Moreover, the sensors' locations on the body could change during limb movements, which could lead to a change in the recorded signal patterns and a lower accuracy of intention prediction. Muscle fatigue can also affect the prediction. In the work by Huang et al. [20], a number of force resistive sensors are mounted on the external shells, which are fixed on the exoskeleton. The inner shells are worn on the user's forearm and upper arm. The obtained signal patterns from these sensors are then analysed and used to control the exoskeleton. Because the sensory system requires direct contact between the inner and outer shells, the user needs to exert a force on the exoskeleton. This can lead to fatigue in the user's arm and reduce the effectiveness of the system. In conclusion, conventional methods still do not recognise human intention efficiently enough and they may cause discomfort for the user during interactions with the exoskeleton because their sensory systems, based on contact sensors, need to be worn on or directly in contact with the user's body.

This research presents a novel approach for human intention recognition based on contactless sensors, which, in contrast with conventional methods, are mounted directly on the exoskeleton and the user's body does not need to be in direct contact with those sensors. The outcome will improve the experience of using exoskeletons. The findings can be extended to detect human intentions for the control of exoskeletons with more degrees of freedom. The preliminary theoretical study of this work was presented by Nguyen et al. [21].

With advantages such as its small size, low mass, and inexpensive cost, the contactless Hall effect sensor has been used widely in non-contact position measurements [22–27]. In this study, the system of Hall effect sensors and a ring permanent magnet with diametrical magnetization is proposed to recognize the human intention. The rest of this paper is organized as follows. Section 2 describes an arrangement of a number of Hall effect sensors and the associated human intention identification algorithm. Section 3 presents the experimental setup. Section 4 discusses the results, and Section 5 draws conclusions.

2. AN ARRANGEMENT OF HALL EFFECT SENSORS AND MAGNETS AND A HUMAN INTENTION IDENTIFICATION ALGORITHM

2.1. An Arrangement of Hall Effect Sensors and Magnets

The arrangement of permanent magnets and Hall effect sensors is presented in Figure 1. There are two semi-ring shaped permanent magnets mounted on the forearm of the user **1**. One piece, **2**, is diametrically magnetised outside the S pole and inside the N pole. On the other hand, another piece, **3**, is diametrically magnetised outside the N pole and inside the S pole. Four linear Hall effect sensors **4**, **5**, **6**, and **7** are mounted in pairs at an angle of 90 degrees on the circular exoskeleton's sensor support, **8**, which is fixed on the exoskeleton and coaxial with the magnets. The thicknesses of the air gaps, **9**, between the Hall effect sensors and magnets are assumed to be equal due to this particular arrangement.

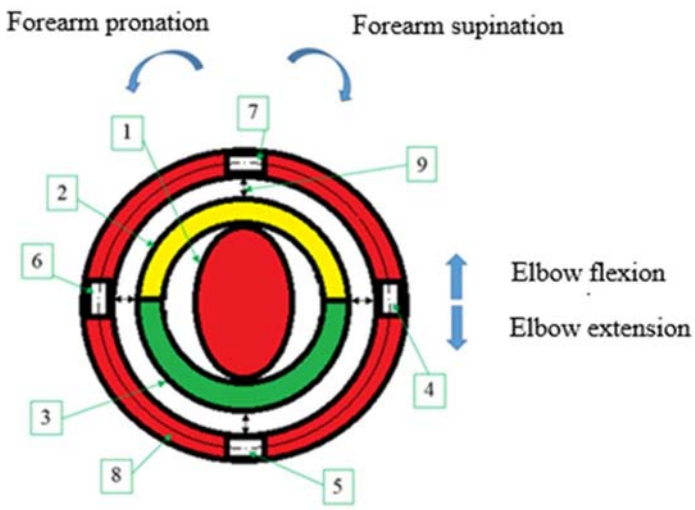

Figure 1. The arrangement system of Hall effect sensors and magnets: **1** — Human forearm; **2** — Semi-ring shape diametrically magnetised S-N; **3** — Semi-ring shape diametrically magnetised N-S; **4**, **5**, **6**, and **7** — linear Hall effect sensors; **8** — Exoskeleton sensors' support; **9** — Air gaps.

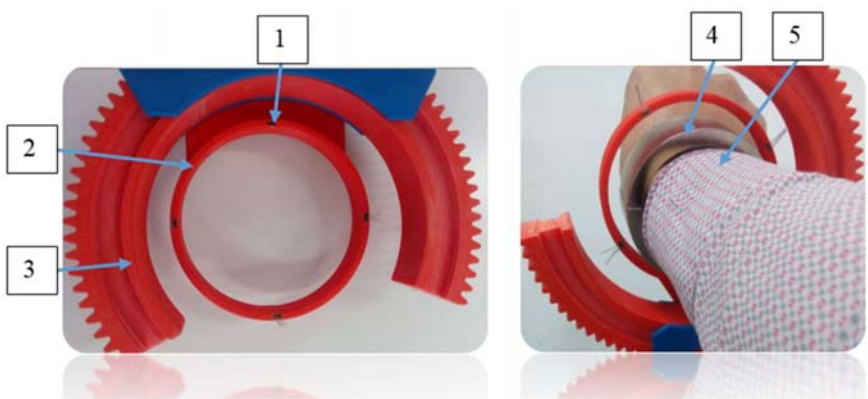

Figure 2. Hall effect sensors in the assembly with the sensors' support: **1** — Hall effect sensor; **2** — Exoskeleton sensors' support; **3** — Forearm big gear; **4** — Permanent magnet; **5** — User's forearm.

Figure 2 depicts the physical assembly of the sensory system including the permanent magnet worn on the user's forearm.

2.2. The Human Intention Identification Algorithm

It is assumed that H_1, H_2, H_3, and H_4 are the received output signals obtained from the Hall effect sensors **4**, **5**, **6** and **7** (Figure 3) respectively, and α is the rotation angle of the user's forearm with magnets. Each of the Hall effect sensors detects only its respective radial part $\mathbf{B_r}$ (more details on the analytical modelling of the magnetic field distribution created by a diametrically magnetised permanent magnet can be found in [28–30]), of the magnetic fields $\mathbf{B}$ (Figure 3), generated by the magnets. Based on the above derived expressions of the magnetic field, the radial component of the magnetic field is the sinusoidal wave of the angle α where its amplitude depends only on the magnet's characteristics and the position of the computed points; hence, the output signals are the sinusoidal waves of the angle α. According to the arrangement, four sinusoidal waveforms, each phase shifted by 90° from its neighbour, are generated [25].

From Figure 3, we have

$$H_1 = A\cos\alpha \tag{1}$$

where A is the constant or the amplitude of the signals of the Hall effect sensors.

According to Figure 3, the following equations are derived:

$$H_2 = A\cos(\alpha + 90^\circ) = -A\sin\alpha \tag{2}$$
$$H_3 = A\cos(\alpha + 180^\circ) = -A\cos\alpha \tag{3}$$
$$H_4 = A\cos(\alpha + 270^\circ) = A\sin\alpha \tag{4}$$

2.2.1. Forearm Rotation Detection

Equations (1)–(4) can be used to derive an expression to calculate the angle α:

$$\alpha = \arctan((H_4 - H_2)/(H_1 - H_3)) \tag{5}$$

The forearm rotation angle can be defined by following Eq. (5), which means that the forearm position can be defined or the pronation/supination movements can be recognized. This system has some advantages, such as it is independent of the signal amplitude and independent of both the temperature and vertical-gap variations of the magnet and temperature drift of the Hall elements. Also, it can cancel any magnetic offsets caused by external magnetic fields [25, 26].

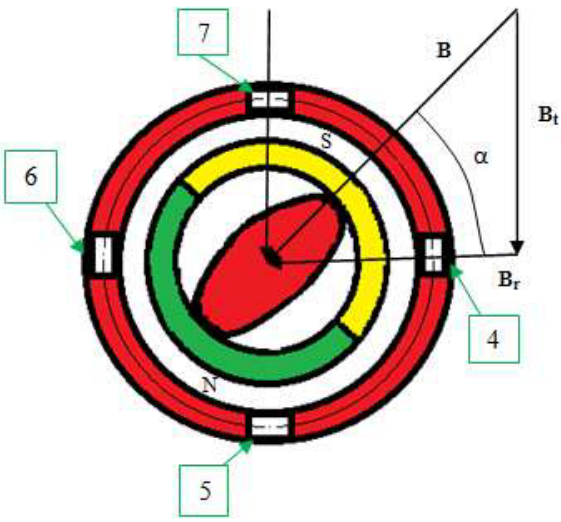

Figure 3. Position of the forearm and magnetic field distribution of the magnets.

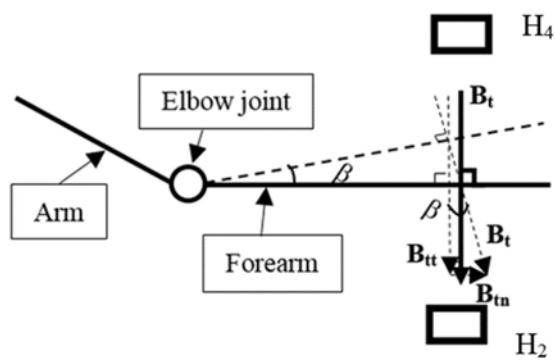

Figure 4. Magnetic distribution during elbow movements.

2.2.2. Elbow Flexion/Extension Motion Recognition

From Eqs. (2) and (4), the absolute values of the output signals from the Hall effect sensors **5** and **7** are equal

$$|H_2| = |H_4| = |A\sin\alpha| \tag{6}$$

when there are no elbow flexion and extension movements (the balanced position).

It is assumed that

$$\varepsilon = |H_4| - |H_2| \tag{7}$$

is the error between the output signals obtained from the Hall effect sensors **7** and **5**.

When the elbow is flexed or extended to a small angle β (Figure 4), the Hall effect sensors **5** and **7** can sense only the radial component $\mathbf{B_{tt}}$, respective to it, of the magnetic fields **B** that have the

magnitude of $B_{tt} = B_t \cos\beta$. Hence, $A_{\mathbf{Btt}} = A_{\mathbf{Bt}} \cos\beta$, where $A_{\mathbf{Btt}}$ and $A_{\mathbf{Bt}}$ are the amplitudes of the signals of a Hall effect sensor sensing $\mathbf{B_{tt}}$ and $\mathbf{B_t}$ at the same position of the forearm, respectively. The following equations can be derived when the forearm with the magnets moves out of the balanced position by the small angle β.

$$|H_2| = |A_2 \cos\beta \sin\alpha| = A_2 |\cos\beta \sin\alpha| \tag{8}$$

$$|H_4| = |A_4 \cos\beta \sin\alpha| = A_4 |\cos\beta \sin\alpha| \tag{9}$$

where A_2 and A_4 are the amplitudes of the output signals obtained from the Hall effect sensors **5** and **7**, when it is assumed that they sense $\mathbf{B_t}$. Hence, the difference between the output signals from these sensors depends only on the difference between the amplitudes A_2 and A_4, which, in turn, depends only on the different air-gaps from the magnets to the Hall effect sensors when the magnets' properties and the surrounding environments are constant. Moreover, the amplitudes A_2 and A_4 increase if the air-gaps decrease, respectively, and vice versa [27, 31].

Subtracting Eq. (8) from Eq. (9) produces

$$\varepsilon = (A_4 - A_2)|\cos\beta \cdot \sin\alpha| \tag{10}$$

From Eq. (10) when $\varepsilon > 0$, $A_4 > A_2$ or the forearm and magnets move closer to sensor **7**, hence elbow flexion is performed.

When $\varepsilon < 0$, $A_4 < A_2$ or the forearm and magnets move closer to sensor **5**, hence elbow extension is performed.

At the initial position of the forearm (Figure 5), the magnetic fields **B** are vertical; hence, the angle $\alpha = 90°$ or

$$|H_1| = |H_3| = |A \cos 90°| = 0$$

and

$$|H_2| = |H_4| = |A \sin 90°| = A$$

A is the amplitude of the output signals.

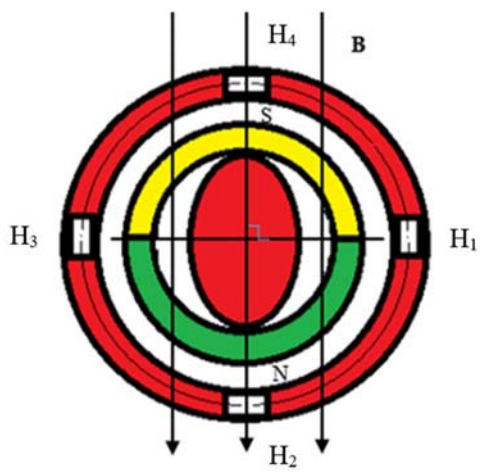

Figure 5. The initial position of the forearm.

Because the maximum average rotation angle of the forearm supination is 86° and the forearm pronation is 61° [32], we can adjust α in the interval [29°, 176°] to avoid $\varepsilon = 0$ independent of A_4–A_2 when $\alpha = 0°$ or $\alpha = 180°$ (zero points).

3. EXPERIMENTAL SETUP

In order to demonstrate the validity of the approach for human intention recognition, a prototype of an assistive elbow and forearm exoskeleton was developed (Figure 6) with the aim to make a lightweight

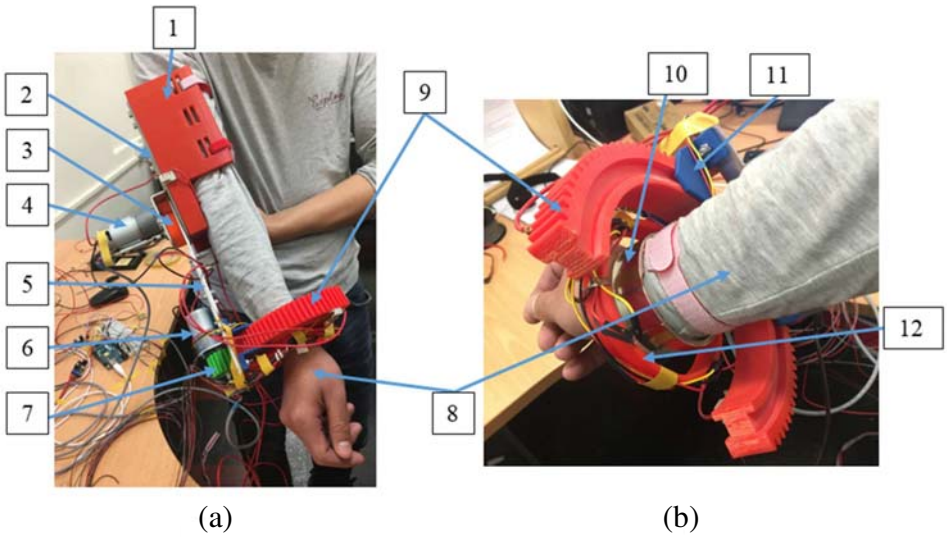

Figure 6. The developed exoskeleton worn by a user: (a) the general view of the exoskeleton worn on the user's upper arm; (b) the view of the user's forearm wearing the ring permanent magnet. **1** — Arm bracer; **2** — Elbow plate; **3** — Elbow gears; **4** — Elbow DC motor; **5** — Forearm plate; **6** — Forearm DC motor; **7** — Forearm pinion gear; **8** — The user's arm; **9** — Forearm larger gear; **10** — Permanent magnet; **11** — Forearm larger gear's support; **12** — Sensors' support.

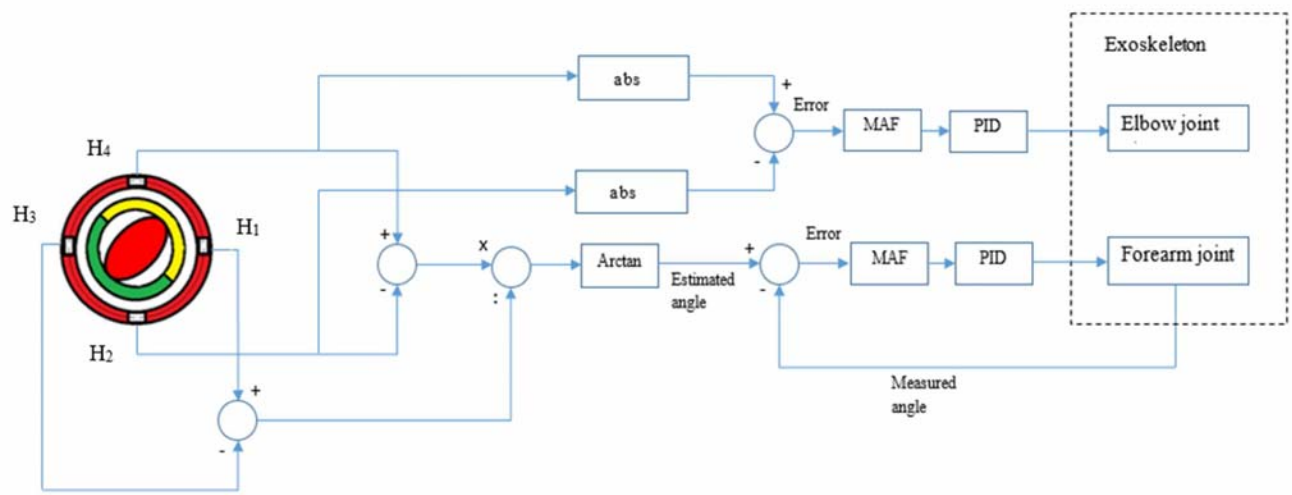

Figure 7. Control architecture of the exoskeleton system: H_1, H_2, H_3 and H_4 — Hall effect sensors; *abs* — absolute; MAF — Moving average filter.

exoskeleton. Some components of the exoskeleton, including the arm brace, elbow gears, forearm pinion gear, forearm larger gear, forearm big gear's support and sensors' support are made of carbon fibre using 3D printing technology. The elbow and forearm plates are made of aluminium alloy. The weight of the ring-shaped permanent magnet used in this experiment is less than 100 grams.

A proportional-integral-derivative (PID) controller was applied to control the exoskeleton, and its coefficients were obtained using manual tuning. The sample rate of the control system was set to 300 Hz. Moving average filters with a window length of 50 were implemented to filter the signals. The control architecture is illustrated in Figure 7. The control program was written using MATLAB/SIMULINK®.

During the experiment, a male with 1.60 m height and 61 kg mass wore the exoskeleton (Figure 6) and performed the elbow and forearm movements in three cases: case 1 — only the forearm rotated; case 2 — only the elbow moved; and, case 3 — the forearm and elbow moved simultaneously.

4. RESULTS AND DISCUSSION

The results obtained from the experiment for the three cases are described as follows.

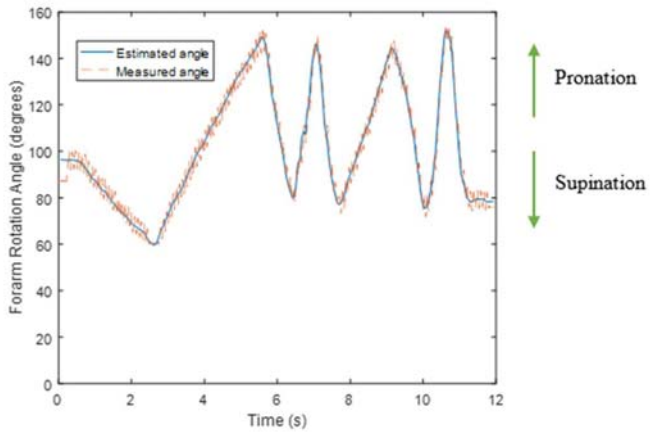

Figure 8. Forearm intended rotation only.

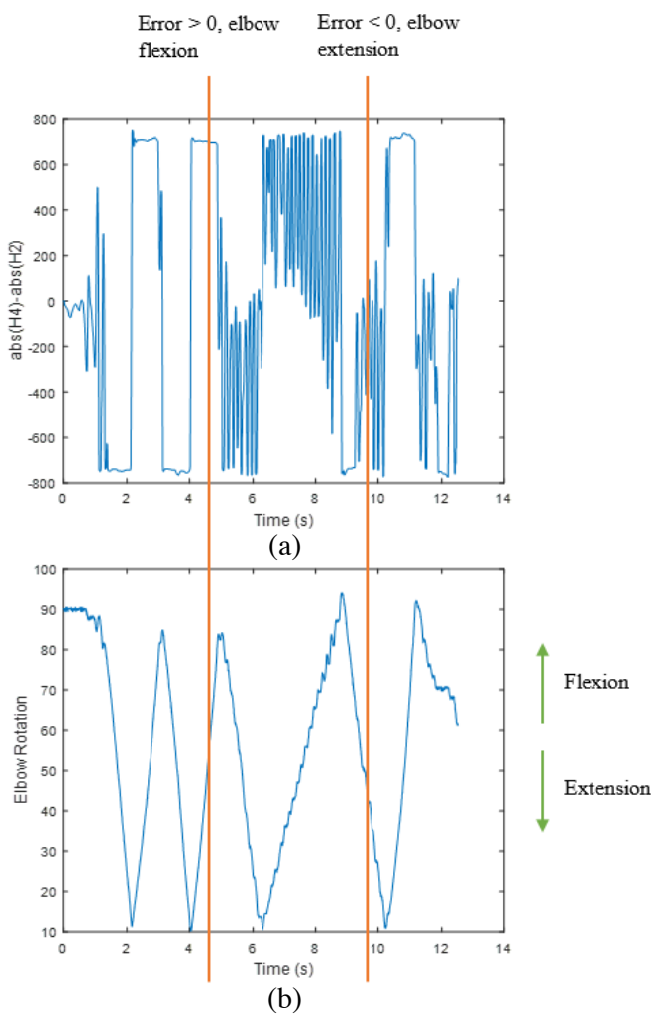

Figure 9. Intended elbow movement only: (a) Error $= abs(H_4) - abs(H_2)$; (b) Elbow (exoskeleton) rotation angle (degrees).

Case 1: Forearm intended rotation only

In the case of intended forearm rotation alone, the user's elbow is considered to be motionless. Figure 8 shows that the sensor arrangement and the human intention recognition algorithm are able to detect

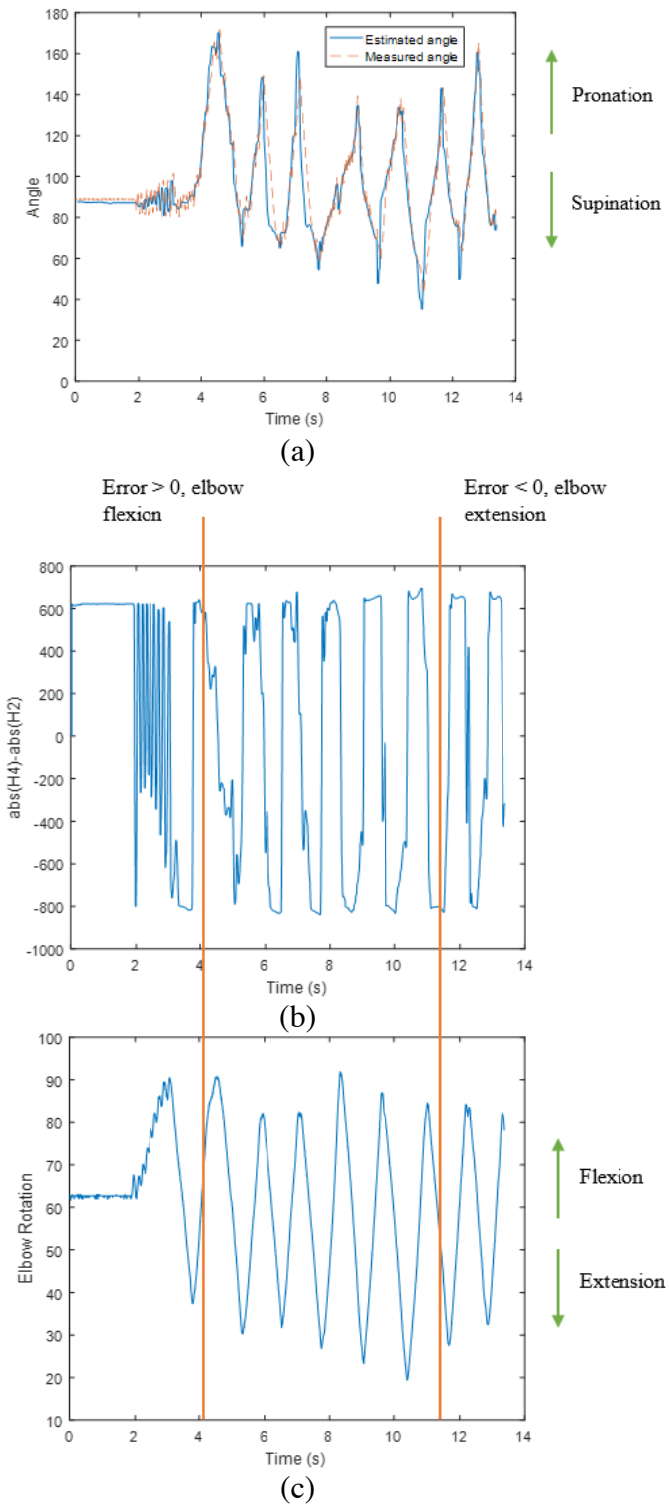

Figure 10. Both forearm and elbow simultaneous movements: (a) Forearm rotation angle (degrees); (b) Error $= abs(H_4) - abs(H_2)$; (c) Elbow (exoskeleton) rotation angle (degrees).

the user's forearm intended rotation (supination/pronation) to control the exoskeleton, as the estimated angle of the forearm is in good agreement with the measured angle.

Case 2: Elbow intended movement only

In the case of an intended elbow movement alone, the user's forearm is considered as remaining motionless. Figure 9(a) shows the error between the absolute value of the output of Hall effect sensor **4** and Hall effect sensor **2** (where error $\varepsilon = abs(H_4) - abs(H_2)$). As illustrated in Figure 9(a) and Figure 9(b) and as proposed by the above theoretical study, when $\varepsilon < 0$ elbow extension was performed and when $\varepsilon > 0$ elbow flexion was performed. The results demonstrate that the sensor arrangement and the human intention recognition algorithm are able to detect the user's intended elbow movement (flexion/extension) to control the exoskeleton.

Case 3: Both intended forearm rotation and intended elbow movements simultaneously

For the case of both intended elbow and forearm movements simultaneously, Figure 10(a) shows that the user's forearm intended motions are recognised as controlling the forearm of the exoskeleton as the estimated angle is in good agreement with the measured angle. While the forearm movements are detected, Figures 10(b) and (c) demonstrate that the elbow motions are also recognised as controlling the exoskeleton, as in case 2; when $\varepsilon < 0$ the elbow extension was performed and when $\varepsilon > 0$, the elbow flexion was performed as proposed by the theoretical study. Therefore, the sensor arrangement and the human intention recognition algorithm is able to detect as well as classify the user's forearm intended rotation and the elbow's intended movements to control the exoskeleton.

5. CONCLUSION

In this research, a novel approach for human intention recognition based on Hall effect sensors and permanent magnets is presented. The experimental results of this study demonstrate that the sensory system of four Hall effect sensors, which are mounted on the exoskeleton, and two semi-ring shaped diametrically magnetised magnets worn on the user's forearm can detect and classify the user's intentions for the control of an assistive exoskeleton, following the human intention identification algorithm. This system lets the user wear an exoskeleton comfortably and easily. Moreover, there is no need to have expert knowledge to help set up the system. As the result of the contactless interaction, the achieved signals are less affected by the wearer's body conditions. These findings can be extended to detect human intentions for control of exoskeletons with more degrees of freedom.

ACKNOWLEDGMENT

The authors would like to thank the School of Mechanical Engineering, University of Adelaide, Australia for providing the equipment, facilities and assistances for this research. We are also grateful to Alison-Jane Hunter for her time helping to edit the English. Van Tai would like to acknowledge the financial support from Thuyloi University according to the Decision #989/QDDHTL.

REFERENCES

1. Rahman, M. H., C. O. Luna, M. Saad, and P. Archambault, "EMG based control of a robotic exoskeleton for shoulder and elbow motion assist," *Jounal of Automation and Control Engineering*, Vol. 3, No. 4, 270–276, 2015.
2. Kiguchi, K. and Y. Hayashi, "An EMG-based control for an upper-limb power-assist exoskeleton robot," *IEEE Transactions on Systems, Man, and Cybernetics, Part B (Cybernetics)*, Vol. 42, No. 4, 1064–1071, Aug. 2012.
3. Andreasen, D. S., S. K. Alien, and D. A. Backus, "Exoskeleton with EMG based active assistance for rehabilitation," *Proceedings of the 9th International Conference on Rehabilitation Robotics, 2005, ICORR 2005*, 333–336, 2005.

4. Lenzi, T., S. M. M. De Rossi, N. Vitiello, and M. C. Carrozza, "Intention-based EMG control for powered exoskeletons," *IEEE Transactions on Biomedical Engineering*, Vol. 59, No. 8, 2180–2190, Aug. 2012.
5. Rahman, M. H., C. O. Luna, M. Saad, and P. Archambault, "Motion control of an exoskeleton robot using electromyogram signals," *Proceedings of Advances in Robotics, Mechatronics and Circuits: 18th International Conference on Circuits (Part of CSCC'14), 2014 International Conference on Mechatronics and Robotics, Structural Analysis (MEROSTA 2014)*, ISBN: 978-1-61804-242-2, 2014.
6. Kiguchi, K., T. Tanaka, and T. Fukuda, "Neuro-fuzzy control of a robotic exoskeleton with EMG signals," *IEEE Transactions on Fuzzy Systems*, Vol. 12, No. 4, 481–490, Aug. 2004.
7. Tang, Z., K. Zhang, S. Sun, Z. Gao, L. Zhang, and Z. Yang, "An upper-limb power-assist exoskeleton using proportional myoelectric control," *Sensors*, Vol. 14, 6677–6694, 2014.
8. Irimia, D. C., M. S. Poboroniuc, F. Serea, A. Baciu, and R. Olaru, "Controlling a FES-EXOSKELETON rehabilitation system by means of brain-computer interface," *Proceedings of International Conference and Exposition on Electrical and Power Engineering (EPE)*, 352–355, Iasi, 2016.
9. Lalitharatne, T. D., K. Teramoto, Y. Hayashi, K. Tamura, and K. Kiguchi, "EEG-based evaluation for perception-assist in upper-limb power-assist exoskeletons," *Proceedings of 2014 World Automation Congress (WAC)*, 307–312, Waikoloa, HI, 2014.
10. Kilicarslan, A., S. Prasad, R. G. Grossman, and J. L. Contreras-Vidal, "High accuracy decoding of user intentions using EEG to control a lower-body exoskeleton," *Proceedings of the 35th Annual International Conference of the IEEE Engineering in Medicine and Biology Society (EMBC)*, 5606–5609, Osaka, 2014.
11. Lee, K., D. Liu, L. Perroud, R. Chavarriaga, and J. del R. Millán, "A brain-controlled exoskeleton with cascaded event-related desynchronization classifiers," *Robotics and Autonomous Systems*, Vol. 90, 15–23, 2017.
12. Li, Z., W. He, C. Yang, S. Qiu, L. Zhang, and C. Y. Su, "Teleoperation control of an exoskeleton robot using brain machine interface and visual compressive sensing," *Proceedings of 2016 12th World Congress on Intelligent Control and Automation (WCICA)*, 1550–1555, Guilin, 2016.
13. Vidaurre, C., C. Klauer, T. Schauer, A. R. Murguialday, and K.-R. Müller, "EEG-based BCI for the linear control of an upper-limb neuroprosthesis," *Medical Engineering & Physics*, Vol. 38, 1195–1204, 2016.
14. Schultz, A. E. and T. A. Kuiken, "Neural interfaces for control of upper limb prostheses: The state of the art and future possibilities," *PM&R*, Vol. 3, No. 1, 55–67, 2011.
15. Noda, T., N. Sugimoto, J. Furukawa, M. A. Sato, S. H. Hyon, and J. Morimoto, "Brain-controlled exoskeleton robot for BMI rehabilitation," *Proceedings of the 12th IEEE-RAS International Conference on Humanoid Robots (Humanoids 2012)*, 21–27, Osaka, 2012.
16. Ammar, L. I., B. Y. Kaddouh, M. K. Mohanna, and I. H. Elhajj, "SAS: SMA aiding sleeve," *Proceedings of the 2010 IEEE International Conference on Robotics and Biomimetics*, 1596–1599, Tianjin, 2010.
17. Ul Islam, M. R. and S. Bai, "Intention detection for dexterous human arm motion with FSR sensor bands," *Proceedings of the Companion of the 2017 ACM/IEEE International Conference on Human-Robot Interaction*, 139–140, Vienna, Austria, 2017.
18. Xiao, Z. G., A. M. Elnady, and C. Menon, "Control an exoskeleton for forearm rotation using FMG," *Proceedings of the 5th IEEERAS/EMBS International Conference on Biomedical Robotics and Biomechatronics*, 591–596, Sao Paulo, 2014.
19. Cho, E., R. Chen, L.-K. Merhi, Z. Xiao, B. Pousett, and C. Menon, "Force myography to control robotic upper extremity prostheses: A feasibility study," *Frontiers in Bioengineering and Biotechnology*, Vol. 4, 18, 2016.
20. Huang, J., W. Huo, W. Xu, S. Mohammed, and Y. Amirat, "Control of upper-limb power-assist exoskeleton using a human-robot interface based on motion intention recognition," *IEEE Transactions on Automation Science and Engineering*, Vol. 12, No. 4, 1257–1270, 2015.

21. Nguyen, V. T., T.-F. Lu, and P. Grimshaw, "Human intention recognition based on contactless sensors to control an elbow and forearm assistive exoskeleton," *Proceedings of the 7th International Conference of Asian Society for Precision Engineering and Nanotechnology (ASPEN 2017)*, ARM-P-06, Seoul, Nov. 2017.
22. Fontana, M., F. Salsedo, and M. Bergamasco, "Novel magnetic sensing approach with improved linearity," *Sensors*, 2013.
23. Wang, S., J. Jin, T. Li, and G. Liu, "High-accuracy magnetic rotary encoder," *System Simulation and Scientific Computing*, 74–82, Springer Berlin Heidelberg, Berlin, 2012.
24. Lee, Y. Y., R. H. Wu, and S. T. Xu, "Applications of linear Hall-effect sensors on angular measurement," *Proceedings of the 2011 IEEE International Conference on Control Applications (CCA)*, 479–482, Denver, CO, 2011.
25. Smirnov, Y., T. Kozina, E. Yurasova, and A. Sokolov, "Analog-to-digital converters of the components of a displacement with the use of microelectronic sine-cosine magnetic encoders," *Measurement Techniques*, Vol. 57, No. 1, 41–46, 2014.
26. Hu, J., J. Zou, F. Xu, Y. Li, and Y. Fu, "An improved PMSM rotor position sensor based on linear hall sensors," *IEEE Transactions on Magnetics*, Vol. 48, No. 11, 3591–3594, 2012.
27. Ramsden, E., *Hall-effect Sensors. Theory and Applications*, 2nd Edition, 272 pages, Newness, Elsevier, 2006.
28. Nguyen, V. T. and T.-F. Lu, "Modelling of magnetic field distributions of elliptical cylinder permanent magnets with diametrical magnetization," *Journal of Magnetism and Magnetic Materials*, Vol. 491, 2019.
29. Nguyen, V. T. and T.-F. Lu, "Analytical expression of the magnetic field created by a permanent magnet with diametrical magnetization," *Progress In Electromagnetics Research C*, Vol. 87, 163–174, 2018.
30. Nguyen, V. T., "Modelling of magnetic fields of permanent magnets with diametrical magnetization," MPhil Thesis, 2019.
31. Jezný, J. and M. Čurilla, "Position measurement with Hall effect sensors," *American Journal of Mechanical Engineering*, Vol. 1, No. 7, 231–235, 2013.
32. Romilly, D. P., C. Anglin, R. G. Gosine, C. Hershler, and S. U. Raschke, "A functional task analysis and motion simulation for the development of a powered upper-limb orthosis," *IEEE Transactions on Rehabilitation Engineering*, Vol. 2, No. 3, 119–129, 1994.